crystals

MDPI

Article

Development of the Amorphous Solid Dispersion of Curcumin: A Rational Selection of Polymers for Enhanced Solubility and Dissolution

Memoona Ishtiaq [1], Sajid Asghar [1], Ikram Ullah Khan [1], Muhammad Shahid Iqbal [2] and Syed Haroon Khalid [1,*]

[1] Department of Pharmaceutics, Faculty of Pharmaceutical Sciences, Government College University, Faisalabad 38000, Pakistan
[2] Department of Clinical Pharmacy, College of Pharmacy, Prince Sattam Bin Abdulaziz University, Al-Kharj 11942, Saudi Arabia
* Correspondence: haroonkhalid80@gmail.com or syedharoonkhalid@gcuf.edu.pk; Tel.: +92-3166752223

Abstract: The goal of this investigation was to determine the effectiveness of hydrophilic polymers in preparing a solid dispersion to enhance the solubility and dissolution of poorly water-soluble drugs, such as curcumin. In order to prepare the solid dispersion, curcumin was uniformly distributed in the polymeric matrix of polyethylene glycol (PEG 6000), hydroxypropyl methyl cellulose (HPMC E5), polyvinyl pyrrolidine (PVP K30), and bovine serum albumin (BSA) using the kneading and solvent evaporation methods. The developed dispersion formulations were characterized for solubility, dissolution, Fourier transform infrared (FTIR), X-ray diffractometry (XRD), scanning electron microscopy (SEM), and differential scanning calorimetry (DSC). Attaining enhanced physical stability with solubility is crucial in the selection of suitable polymer types and ratios. The optimized HPMC E5 and PVP based dispersion displayed 4.3 and 2.8 times greater solubility compared to the pure drug, respectively. The SEM also showed the optimized HPMC-based dispersion was smoother in comparison to the PVP-based dispersion. The XRD and DSC validated the successful modification of the crystal structure of curcumin resulting in the enhancement of its solubility and dissolution. In conclusion, the HPMC E5 formulation was the optimal candidate to create solid amorphous dispersions of curcumin, which might be employed as an effective delivery system.

Keywords: curcumin; solid dispersion; polymers; solubility; dissolution

Citation: Ishtiaq, M.; Asghar, S.; Khan, I.U.; Iqbal, M.S.; Khalid, S.H. Development of the Amorphous Solid Dispersion of Curcumin: A Rational Selection of Polymers for Enhanced Solubility and Dissolution. *Crystals* **2022**, *12*, 1606. https://doi.org/10.3390/cryst12111606

Academic Editors: Krzysztof Szymkiewicz and Marek Goral

Received: 17 October 2022
Accepted: 7 November 2022
Published: 10 November 2022

1. Introduction

The most crucial physicochemical factor influencing bioavailability is solubility. Recent advancements in drug discovery approaches have resulted in a growing number of drugs with limited aqueous solubility. According to one estimate, nearly forty percent of the marketed drugs exhibit poor solubility [1]. For this purpose, overcoming poor aqueous solubility remains among the most researched areas. In an attempt to resolve this issue, numerous strategies including the size reduction, salt formation, vesicular delivery, and solid dispersion have been employed [2]. Amongst these, solid dispersion is an effective strategy, as uniformly dispersing an active constituent in an inert matrix, as well as the amorphous state of the active constituent, facilitate transient drug solubilization [3].

As carriers, hydrophilic polymers are well known for essentially improving the solubility of hydrophobic drugs. The role of these carriers is to add stability and solubility and significantly alter the rate of dissolution. Even though a number of polymers have shown their efficacy in increasing solubility, the efficiency of solid dispersion is heavily dependent on the carrier used [4]. Hence, the effects of the incorporation of bovine serum albumin (BSA), PEG 6000, HPMC E5, and PVP K30 were studied in this investigation. The choice of polymers was made based on their safety, efficacy, and accessibility. All the polymers

included in the study were generally recommended as safe (Grass), approved by the Food and Drug Administration (FDA), and easily available.

As the most common protein, BSA has been regarded as soluble, biocompatible, and an extremely stable excipient. The unique capacity of albumin to produce reversible ligand complexes is primarily responsible for its solubility enhancing characteristics [5]. Ligands are typically attached at two binding sites predominantly through both electrostatic and hydrophobic bonds. Furthermore, the presence of positive charge on these sites also facilitates anionic bonding [6]. Depending upon the wettability, both polyethylene glycols and HPMC also aid in improving the solubility of numerous ligands; however, the main reason behind the higher dissolution and prolonged super saturation of these dispersion formulations is the shift to an amorphous state and crystallization inhibition [7–9]. Similarly, for polymers such as PVP, the drug loses it crystal structure and changes to an amorphous state; however, the concentration of the carrier is decisive in this aspect [10]. Hence, several different concentration ratios of polymers were optimized. Apart from the aforementioned mechanisms, decreasing the overall size distribution also accounts for improved solubility. Even though size reduction can be acquired through different solid dispersion techniques, the aim of improving dissolution is not achieved by this alone, since dissolution involves an interplay between the amorphous state and size [11,12].

Curcumin, a lipophilic polyphenol drug obtained from the plant curcuma longa, has been employed for centuries for its anti-inflammatory, antibacterial, antioxidant, anticancer, and hypoglycemic effects. Despite the versatile applicability of curcumin, its poor aqueous solubility imparts numerous limitations in its clinical advancement [13].

In this investigation, different solid dispersion formulations of curcumin and hydrophilic polymers were formulated by kneading and solvent evaporation. Both methods were selected due to their simplicity, cost effectiveness, and ease of scalability. In addition to polymer selection, the polymer ratio is also a significant aspect of solid dispersion that can affect the solubility and stability of the curcumin. Therefore, the solubility, crystallinity, thermal behavior, and release of the solid dispersion were examined in accordance with the type and amount of the polymeric matrix, which to our knowledge has not been investigated before.

Hence, the purpose of the study was to develop and explore the effect of PEG 6000, HPMC E5, PVP K30, and BSA-based curcumin solid dispersion formulation in enhancing the solubility and dissolution of poorly soluble curcumin. Depending on the type of polymer kneading and solvent evaporation, the techniques were combined with an amount of the polymeric carrier, and the physicochemical properties of the prepared formulations were evaluated using scanning electron microscopy (SEM), Fourier transform infrared (FTIR), differential scanning calorimetry (DSC), and X-ray powder diffraction (XRD).

2. Materials and Methods

2.1. Materials

Curcumin (≥95% curcuminoids) was purchased from Natural Remedies Pvt Limited, Bangalore, India. Bovine serum albumin (BSA), polyethylene glycol 6000 (PEG 6000), hydroxypropylmethyl cellulose E5 (HPMC E5), and polyvinylpyrrolidone K 30 (PVP K30), were supplied by ISP Technologies Inc. Wayne, NJ, USA). The materials were used as received.

2.2. Preparation of Solid Dispersions

As indicated in Table 1, the solid dispersion of curcumin and different hydrophilic polymers, namely BSA, PEG 6000, HPMC E5, and PVP K30, were synthesized in the following weight ratios of 1:0, 1:1, 1:2, 1:4, and 1:8. Overall, two techniques were employed in order to form the dispersions.

Table 1. Curcumin and carriers (PEG 6000, HPMC E5, PVP K30, and BSA) at different ratios.

Code	CUR: Polymer Ratio
CUR	CUR: No Polymer (1.0:0.0)
CUR: PEG 6000 1:1	CUR: PEG 6000 (1.0:1.0)
CUR: PEG 6000 1:2	CUR: PEG 6000 (1.0:2.0)
CUR: PEG 6000 1:4	CUR: PEG 6000 (1.0:4.0)
CUR: PEG 6000 1:8	CUR: PEG 6000 (1.0:8.0)
CUR: HPMC E5 1:1	CUR: HPMC E5 (1.0:1.0)
CUR: HPMC E5 1:2	CUR: HPMC E5 (1.0:2.0)
CUR: HPMC E5 1:4	CUR: HPMC E5 (1.0:4.0)
CUR: HPMC E5 1:8	CUR: HPMC -E5 (1.0:8.0)
CUR: PVP K30 1:1	CUR: PVP K30 (1.0:1.0)
CUR: PVP K30 1:2	CUR: PVP K30 (1.0:2.0)
CUR: PVP K30 1:4	CUR: PVP K30 (1.0:4.0)
CUR: PVP K30 1:8	CUR: PVP K30 (1.0:8.0)
CUR: BSA 1:1	CUR: BSA (1.0:1.0)
CUR: BSA 1:2	CUR: BSA (1.0:2.0)
CUR: BSA 1:4	CUR: BSA (1.0:4.0)
CUR: BSA 1:8	CUR: BSA (1.0:8.0)

The kneading method consisted of mixing the accurately weighed drug and polymers followed by kneading in a pestle and mortar for 60 min. The solvent mixture used for kneading was ethanol and water (1:1). The kneaded mixture was dried in an oven at 45 °C for twenty-four hours, then crushed, sieved, and stored.

For solvent evaporation, both curcumin and the polymers were individually dissolved in ethanol and water, respectively. With the aid of a magnetic stirrer, both solutions were thoroughly stirred on a hot plate for approximately fifteen minutes. In order to evaporate the solvent, the resultant mixture was first placed in a rotary evaporator, followed by a hot air oven for twenty-four hours. The obtained dried mass was crushed, sieved, and stored for further application.

2.3. Solubility Study

In order to check the solubility, a surplus amount of the drug and solid dispersions was added to distilled water (10 mL) and mixed for approximately 3 min using a vortex mixer. After mixing, all the samples were placed in shaking water at 25 °C ± 2 °C and 120 rpm for 3 days. The obtained supernatant was then filtered using a 0.45 µm membrane filter and analyzed spectrophotometrically (UV-1700, Shimadzu, Japan) [14]. Each experiment was conducted thrice.

2.4. In Vitro Dissolution Studies

For the dissolution studies, a USP apparatus II or paddle method (PTWS 3CE, Pharmatest, Germany) was employed with dissolution media consisting of water and a paddle moving at a velocity of 100 rpm. The temperature of the dissolution media was maintained at 37.0 ± 0.5 °C. Each vessel contained an equal amount of the drug (10 mg) and was sampled (5 mL) at intervals of 5, 10, 20, 30, 40, 50, and 60 min. Each sample was then filtered and analyzed using a UV spectrophotometer (UV-1700, Shimadzu, Japan) at a wavelength of 370 nm. Furthermore, in order to maintain sink conditions, each sample taken was then substituted with an equal amount of the dissolution media [15].

2.5. Scanning Electron Microscopy (SEM)

The surface morphology of both the drug and solid dispersions was observed using scanning electron microscopy (JSM-6480, Tokyo, Japan). Prior to imaging, each sample was stammered in gold coating.

2.6. Fourier Transform Infrared Spectroscopy (FTIR)

Both the drug and solid dispersion were analyzed by means of a potassium bromide disk (BRUKER-Tensor II-ALPHA, Bremen, Germany) starting from 400 to 4000 cm^{-1} for probable suggestions regarding the structure and functional groups.

2.7. Differential Scanning Calorimetry (DSC)

Differential scanning calorimetry was measured using a Universal V4.2E TA Instruments (Newcastle, DE, USA). Each sample, consisting of 3 to 10 mg of curcumin, was placed in an aluminum pan and analyzed from 20 to 400 °C under nitrogen flow at a velocity of 10 °C/min.

2.8. Powder X-ray Diffraction Study (XRD)

To access the structural information of the solid dispersion, an X-ray diffractometer (Bruker D-8 Advance, Germany) equipped with a graphite monochromator and Cu-Kα radiation was used. Each sample was scanned over an array of 5 to 80° at a rate of 5°/min followed by additions of 0.05° at 40 KV and a 30 mA current.

2.9. Statistical Analysis

The data were displayed as the mean ± S.D. All statistical calculations were carried out using SPSS version 20. IBM, Chicago, IL, USA.

3. Results and Discussion

3.1. Solubility Studies

The solubility statistics of CUR and its solid dispersions are exhibited in Figure 1. The incorporation of the hydrophilic polymers resulted in a substantial increase in the solubilization [16]. Overall, the addition of the HPMC E5 resulted in superior solubility closely followed by the PVP K30. Meanwhile, the BSA and PEG 6000 presented comparatively reduced solubility values even at higher concentrations (1:8) [17]. These findings confirm the selection of a polymer to be a key element in enhancing the solubility. Consequently, only HPMC E5 and PVP K30 were selected for further investigation. Typically, an increase in the proportion of a hydrophilic polymer is capable of enhancing the solubility of a solid dispersion; however, in this investigation, the degree of solubility ameliorated only up to the ratio of 1:4 (drug:polymer), and any additional increase in polymer did not demonstrate any higher solubility. Thus, the drug polymer solid dispersions at a ratio of 1:8 were not included in further investigations. Although the amorphous form of HPMC E5 and PVP K30 polymer-based dispersions is the primary mechanism for improved solubilization, the inclusion of both hydroxyl and ether groups in the structural makeup of HPMC might have resulted in further enhanced drug solubility [18,19].

3.2. In Vitro Dissolution Study

The in vitro dissolution kinetics of both the curcumin and prepared HPMC E5 and PVP K30 solid dispersion are displayed in Figure 2. In comparison to the pure drug, the rate of the dissolution of curcumin with HPMC E5 and PVP K30 indicated a prominent increase in the dissolution up to approximately 72 and 57%, respectively, at 60 min. This was attributed to the improved wettability as well as the dispersibility potential of the CUR in the solid dispersion prepared by the hydrophilic polymers. The hydrophilic polymers involved in preparing the dispersion formulations help to increase the wettability and decrease the surface tension between the lipophilic drug and dissolution medium [20,21]. In terms of the polymer, the HPMC E5-based dispersions presented higher rates of dissolution

in comparison to the PVP K30. For the HPMC E5-based dispersion, the main reason for its enhanced dissolution was assumed to be the crystal inhibition capability of HPMC; since HPMC, in contrast to PVP, is a stronger precipitation inhibitor, it explains the superior rate of dissolution [19,22]. Furthermore, since an increase in the hydrophilic polymer resulted in an increase in the dissolution, the drug/polymer ratios of 1:2 and 1:4 were chosen for subsequent study. Similarly, the techniques used for the preparation of the solid dispersion also affected the dissolution rate. In this regard, the dissolution rate of the CUR dispersed in the PVP K30 matrix by kneading and in the HPMC E5 matrix by the solvent evaporation techniques was found to be higher.

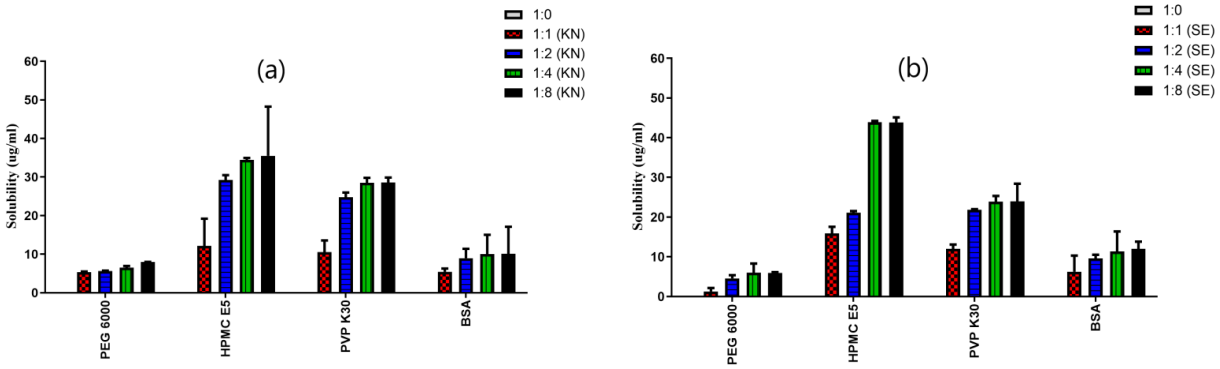

Figure 1. Solubility data of CUR, CUR:PEG 6000, CUR: HPMC E5, CUR:PVP K30, and CUR:BSA by the kneading (**a**) and solvent evaporation (**b**) methods. Mean ± SD, N = 3.

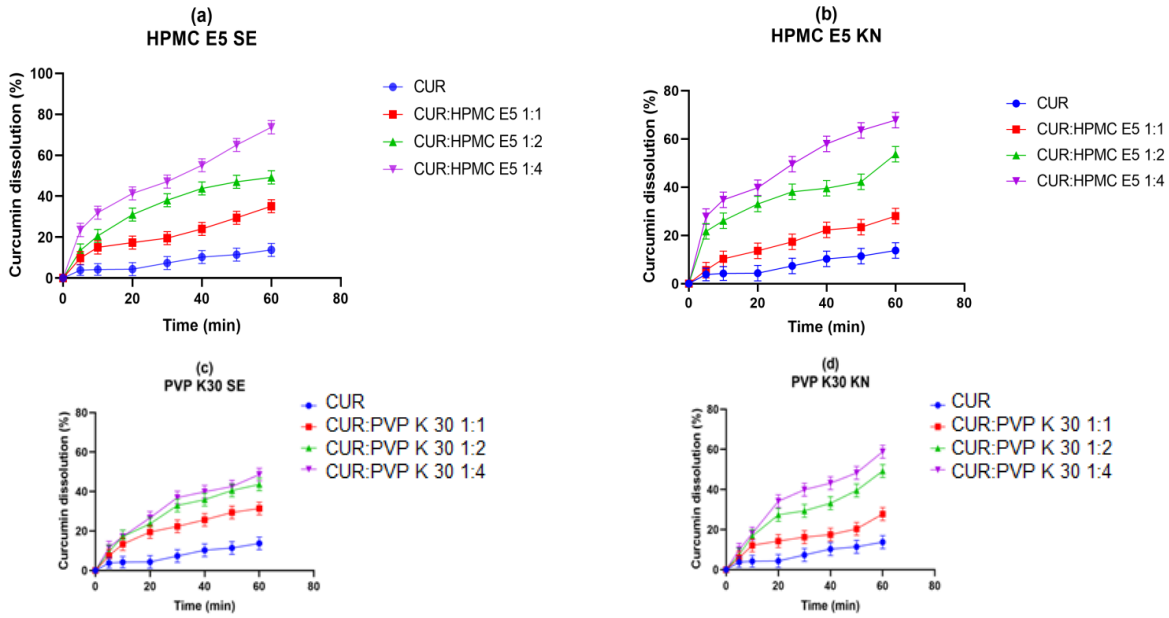

Figure 2. Mean dissolution profile of CUR and solid dispersions with (**a**) HPMC E5 SE, (**b**) HPMC E5 KN, (**c**) PVP K30 SE, and (**d**) PVP K30 KN. Mean ± SD, N = 3.

3.3. Scanning Electron Microscopy (SEM)

SEM images of the curcumin powder and its solid dispersions with HPMC E5 and PVP K30 are presented in Figure 3A,B. The CUR exhibited flat broken particles with an irregular shape, while the pure HPMC appeared as cylindrical-shaped particles (Figure 3(Ab)), and the PVP consisted of spheres with concave depressions (Figure 3(Bb)). For the solid dispersions, the CUR was found to be dispersed as well as deposited on the surface of the hydrophilic polymers. Moreover, the possibility of the disappearance of the original structure of the CUR in these dispersions also confirmed the change in structure. In

addition, the smoother surface of the HPMC-based dispersions in comparison to the PVP was also suggestive of its higher solubility.

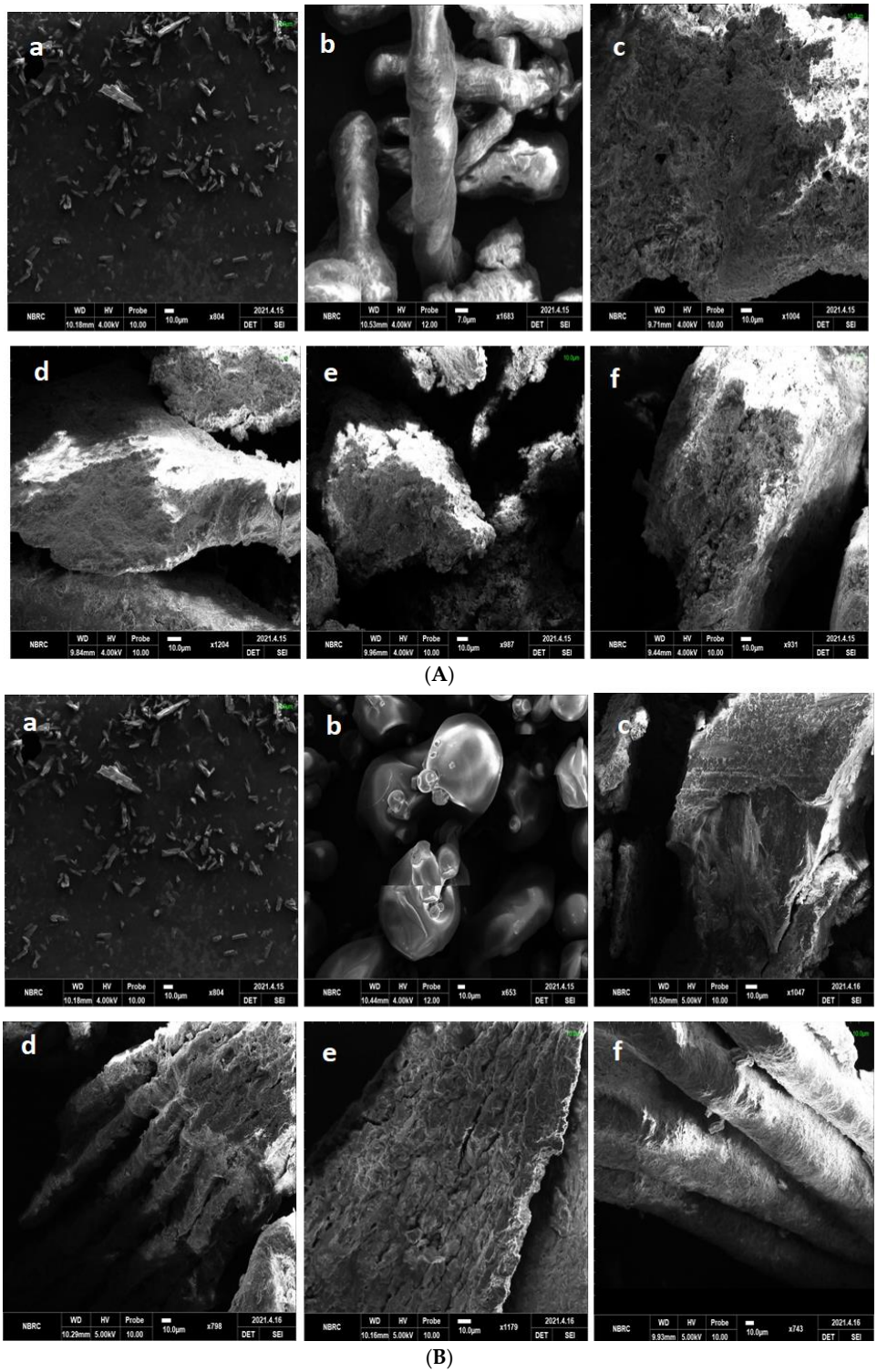

Figure 3. (**A**). SEM images of pure curcumin (**a**), HPMC E5 (**b**), CUR:HPMC E5 1:2 KN (**c**), CUR: HPMC E5 1:4 KN (**d**), CUR:HPMC E5 1:2 SE (**e**), and CUR: HPMC E5 1:4 SE (**f**). (**B**). SEM images of pure curcumin (**a**), PVP K30 (**b**), CUR:PVP K30 1:2 KN (**c**), CUR:PVP K30 1:4 KN (**d**), CUR:PVP K30 1:2 SE (**e**), and CUR:PVP K30 1:4 SE (**f**).

3.4. FTIR

Figure 4A,B illustrates the FTIR spectra of the curcumin and its solid dispersions with HPMC E5 and PVP K30, respectively. The FTIR spectra of curcumin was found to be in accordance with previous studies [23–25]. The prominent spectrum of curcumin was as follows: 3589, 1608, and 1259 cm^{-1}. Generally, the stretching region of the hydroxyl group, O–H was shown at the band range of 3200–3600 cm^{-1}. The band for the carbonyl group (C=O) appeared at the band range of 1620–1650 cm^{-1}. The sharp peak was noticed for the carbonyl group in curcumin at 1608 cm^{-1}.

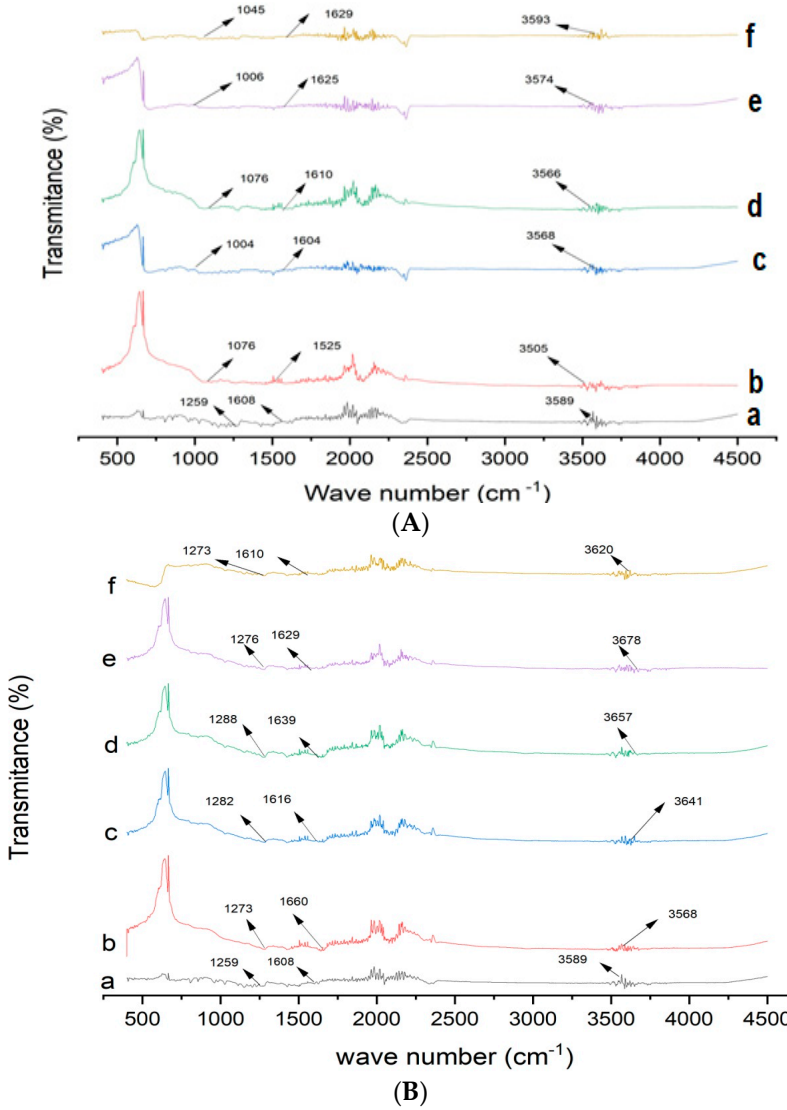

Figure 4. (**A**) FTIR spectra of (a) curcumin, (b) HPMC E5, (c) CUR:HPMC E5 1:2KN, (d) CUR:HPMC 1:4 KN, (e) CUR:HPMC 1:2 SE, and (f) CUR:HPMC 1:4 SE. (**B**). FTIR spectra of (a) pure curcumin, (b) PVP K30, (c) CUR:PVP K30 1:2 KN, (d) CUR:PVP K30 1:4 KN, (e) CUR:PVP K30 1:2 SE, and (f) CUR:PVP K30 1:4 SE.

The spectrum of the pure HPMC E5 showed the characteristic broad absorption band of the O–H group, which was evident in the range of 3100–3600 cm^{-1}. This was in good agreement with the published data on the polymer. The FTIR spectrum of the HPMC E5, shown in Figure 4b, displayed characteristics peaks at 3505, 1525, and 1076 cm^{-1}, revealing the presence of the hydroxyl group (OH) stretching, the vibration of the hydroxyl group (OH), and the C–O group stretching, respectively. The spectrum of HPMC E5 was confirmed through a literature study performed by Akhlaq et al. [26,27].

There were shift wave numbers of -OH stretching at 3568, 3566, 3574, and 3593 cm^{-1} for the solid dispersion at 1:2 and 1:4 ratios, respectively. These wavelength shifts were still within the range of O-H. Moreover, the shift wave numbers of the C=O group of solid dispersion 1:2 and 1:4 (KN and SE methods) were at 1604 cm^{-1}, 1610 cm^{-1}, 1625 cm^{-1}, and 1629 cm^{-1}, respectively.

The FTIR spectrum of the pure PVP K30 produced a characteristic absorption band at 1660 cm^{-1}, which can be attributed to the carbonyl group. The very broad band at 3568 cm^{-1} was due to the O-H stretching vibrations of the absorbed water. The PVP K30 exhibited an obvious absorption peak near 1273 cm^{-1}, which belonged to the O-H in-plane bending vibration. The spectrum of the PVP K30 was confirmed through literature studies performed by Gamal and Ramy (2014) [28,29].

For the SD of the drug with PVP K30, the infrared spectra of the solid dispersions clearly showed the absorption bands, illustrating the presence of curcumin and PVP K30 (Figure 4B(c–f)). There were shift wave numbers of O-H stretching at 3641, 3657, 3678, and 3620 cm^{-1} for the solid dispersion at the 1:2 and 1:4 ratios, respectively. This wavelength shift was still within the range of O-H. Moreover, the shift wave numbers of the C=O group of the solid dispersion 1:2 and 1:4 (KN and SE methods) were at 1616 cm^{-1}, 1639 cm^{-1}, 1629 cm^{-1}, and 1610 cm^{-1}, respectively.

Thus, there was no new functional group observed, which indicated no chemical interaction occurred between the curcumin, HPMC E5, and PVP K30 in the solid dispersion at all ratios. This result was anticipated, since the preparation of the solid dispersion was not to produce a new substance but to modify the physicochemical properties [30].

3.5. Differential Scanning Calorimetry

The DSC curves were obtained to confirm the effect of the temperature on the curcumin formulations. The DSC of the pure curcumin displayed a single endothermic peak at 188 °C with an enthalpy of fusion of 103.5 J/g analogous to the melting point of curcumin. The HPMC E5 showed an endothermic peak at 88 °C (Figure 5(Ab)), while the PVP K30 (Figure 4(Bb)) exhibited two endothermic peaks at 114 and 139 °C. The DSC curves of the curcumin and polymers were in agreement with the previously published studies [23,31–33]. In terms of the thermal behavior, both the HPMC E5- and PVP K30-based dispersions overall revealed an endothermic peak of curcumin but with a decline in the intensity of peaks, a reduction in enthalpy from 103.5 to 6.10 J/g, as well as shifting of the melting temperature away from the characteristic curcumin peak signifying the presence of the drug in amorphous form. The intensity of the characteristic peaks obtained for the HPMC-based dispersion from the solvent evaporation method (Figure 5(Ae,f)) and the PVP-based dispersions from the kneading method (Figure 5(Bc,d)) was markedly reduced with CUR:PVP 1:4 KN and CUR:HPMC 1:4 SE (Figure 5(A,Bd)) exclusive of any peak, confirming the uniform distribution as well as the fully amorphous state of curcumin in the polymeric matrix.

3.6. X-ray Diffraction

The XRD patterns were obtained to validate the molecular structure of the curcumin in the HPMC/PVP-based dispersions (Figure 6A,B). The pure curcumin exhibited a diffraction pattern with characteristic sharp peaks between 7 and 27° at a value of 2θ implying the existence of curcumin in crystalline form [24,34]. Meanwhile, the HPMC E5 (Figure 6(Ab)) and PVP K30 (Figure 6(Bb)), being highly amorphous, presented no such peaks [35]. Similarly, the diffractograms of the solid dispersions also displayed a pattern without any sharp peaks of curcumin confirming the ability of the HPMC- and PVP-based solid dispersion to change the crystallinity of the curcumin to a slightly crystalline or amorphous state. Moreover, it is also notable that the sharpness of the peaks declined upon increasing the CUR–polymer ratio from 1:2 to 1:4 resulting in a more amorphous and less crystalline lattice. Based on the polymer, this modification from crystalline to amorphous form is a major component in increasing the solubility as well as the dissolution. These findings also

confirm the effectiveness of the kneading and solvent evaporation methods in enhancing the solubility by changing the crystal structure of curcumin to an amorphous form.

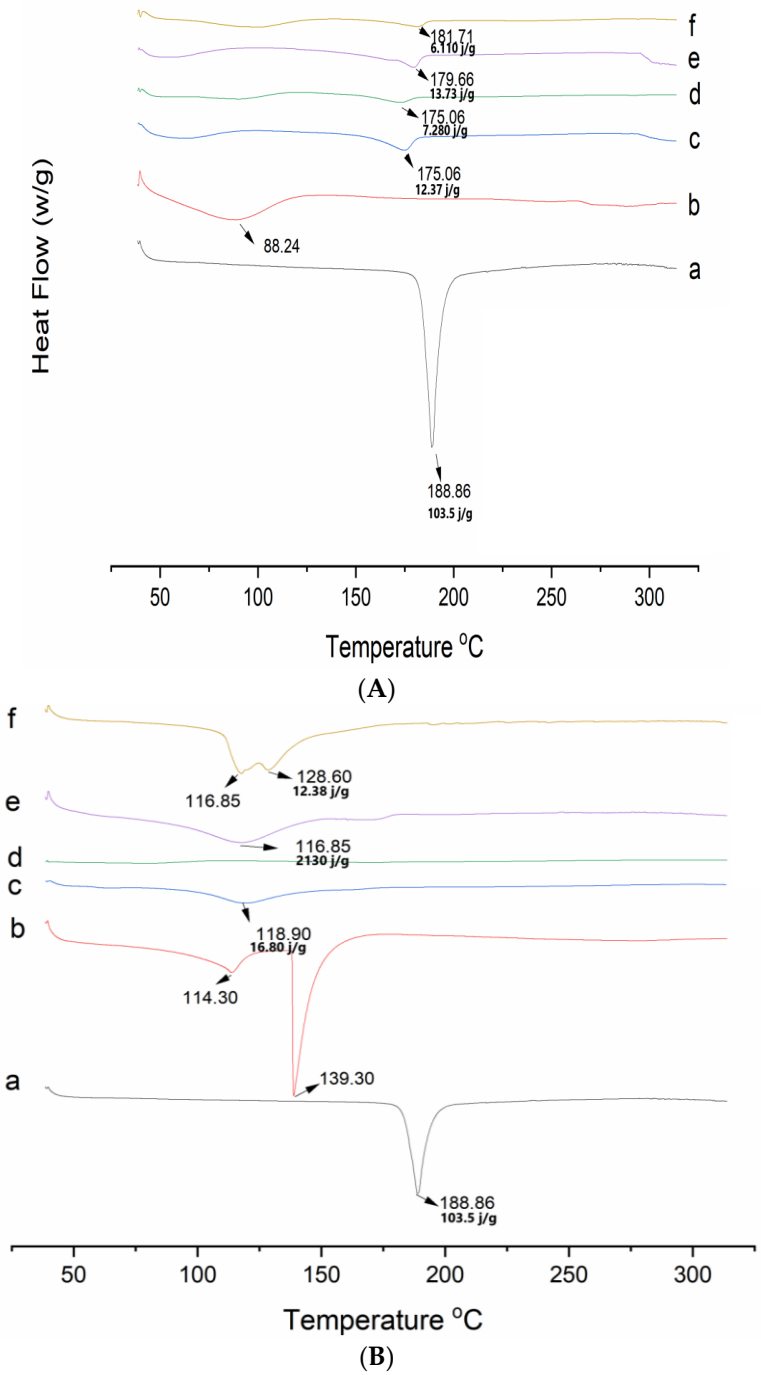

Figure 5. (**A**). DSC curves of (a) pure curcumin, (b) HPMC E5, (c) CUR:HPMC E5 1:2KN, (d) CUR:HPMC E5 1:4 KN, (e) CUR:HPMC E5 1:2 SE, and (f) CUR: HPMC E5 1:4 SE. (**B**). DSC curves of (a) pure curcumin, (b) PVP K30, (c) CUR:PVP K30 1:2 KN, (d) CUR:PVP K30 1:4 KN, (e) CUR:PVP K30 1:2 SE, and (f) CUR:PVP K30 1:4 SE.

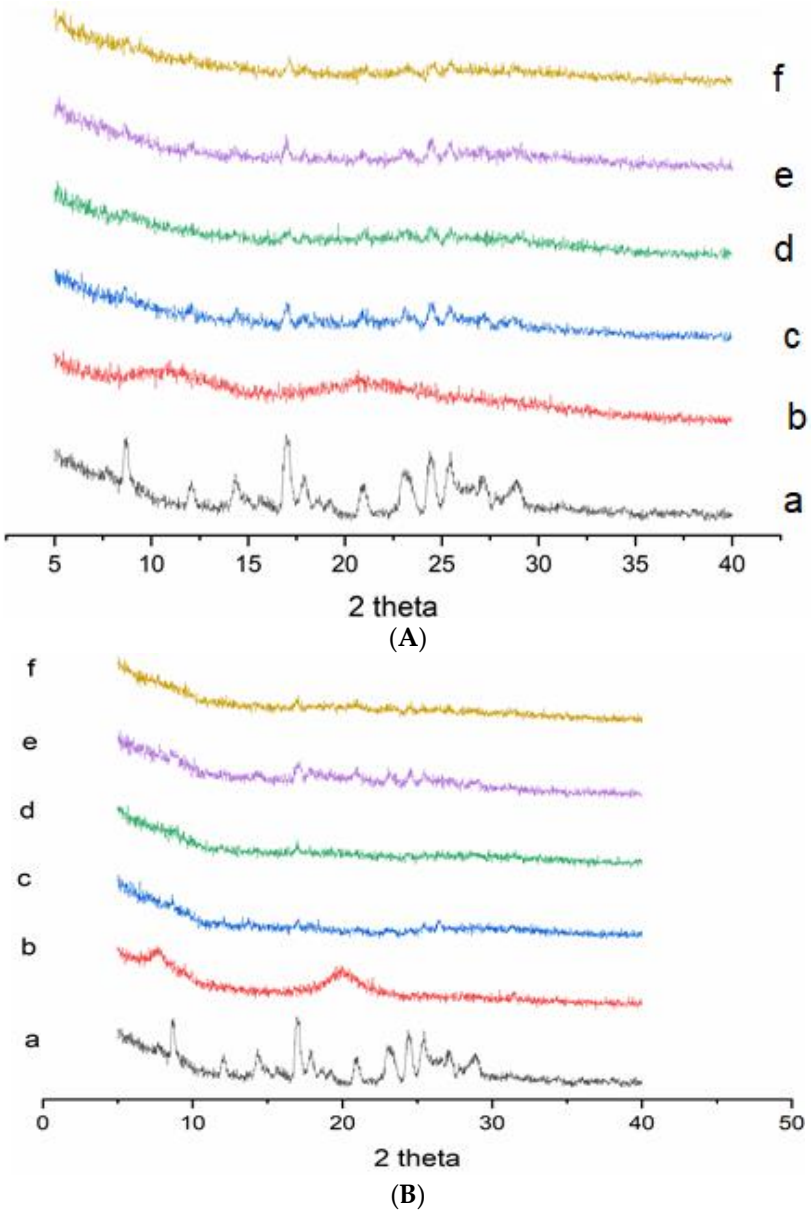

Figure 6. (**A**). Diffractograms of (a) pure curcumin, (b) HPMC E5, (c) CUR:HPMC E5 1:2 KN, (d) CUR: HPMC 1:4 KN, (e) CUR:HPMC 1:2 SE, and (f) CUR: HPMC 1:4 SE. (**B**). Diffractograms of (a) pure curcumin, (b) PVP K30, (c) CUR:PVP K30 1:2 KN, (d) CUR:PVP K30 1:4 KN, (e) CUR:PVP K30 1:2 SE, and (f) CUR:PVP K30 1:4 SE.

4. Conclusions

As evidenced by the findings of the physicochemical evaluations, the solid-state amorphous dispersions consisting of curcumin and hydrophilic polymers, including HPMC E5 and PVP K30, for enhancing the solubility of curcumin were successfully developed. In addition to the type, the ratio of the hydrophilic polymers and the method of preparation also markedly affected the overall solubility, rate of dissolution, and physicochemical evaluations. In particular, the CUR: HPMC E5 (1:4 SE) and CUR: PVP K30 (1:4 KN) exhibited higher solubility and dissolution.

Author Contributions: Conceptualization, S.A. and S.H.K.; Data curation, M.S.I.; Formal analysis, M.I. and S.H.K.; Funding acquisition, M.I., M.S.I. and S.H.K.; Investigation, M.I., S.A. and S.H.K.; Methodology, S.A. and S.H.K.; Project administration, S.H.K.; Resources, I.U.K. and M.S.I.; Software, S.H.K.; Validation, I.U.K.; Visualization, I.U.K.; Writing—original draft, M.I.; Writing—review and editing, S.H.K. All authors have read and agreed to the published version of the manuscript.

Funding: This research received no external funding.

Data Availability Statement: Data is contained within the article.

Conflicts of Interest: The authors declare no conflict of interest.

References

1. Savjani, K.T.; Gajjar, A.K.; Savjani, J.K. Drug solubility: Importance and enhancement techniques. *Int. Sch. Res. Not.* **2012**, *2012*, 195727. [CrossRef] [PubMed]
2. Da Silva, F.L.O.; Marques, M.B.d.; Kato, K.C.; Carneiro, G. Nanonization techniques to overcome poor water-solubility with drugs. *Expert Opin. Drug Discov.* **2020**, *15*, 853–864. [CrossRef] [PubMed]
3. Sareen, S.; Joseph, L.; Mathew, G. Improvement in solubility of poor water-soluble drugs by solid dispersion. *Int. J. Pharm. Investig.* **2012**, *2*, 12. [CrossRef] [PubMed]
4. Huang, Y.; Dai, W.-G. Fundamental aspects of solid dispersion technology for poorly soluble drugs. *Acta Pharm. Sin. B* **2014**, *4*, 18–25. [CrossRef] [PubMed]
5. Topală, T.; Bodoki, A.; Oprean, L.; Oprean, R. Bovine serum albumin interactions with metal complexes. *Clujul Med.* **2014**, *87*, 215. [CrossRef] [PubMed]
6. Urien, S.; Tillement, J.-P.; Barré, J. The significance of plasma-protein binding in drug research. In *Pharmacokinetic Optimization in Drug Research: Biological, Physicochemical, and Computational Strategies*; Wiley Verlag: Zurich, Switzerland, 2001; pp. 189–197.
7. Setyawan, D.; Fadhil, A.A.; Juwita, D.; Yusuf, H.; Sari, R. Enhancement of solubility and dissolution rate of quercetin with solid dispersion system formation using hydroxypropyl methyl cellulose matrix. *Thai J. Pharm. Sci.* **2017**, *41*, 112–116.
8. Iemtsev, A.; Hassouna, F.; Mathers, A.; Klajmon, M.; Dendisová, M.; Malinová, L.; Školáková, T.; Fulem, M. Physical stability of hydroxypropyl methylcellulose-based amorphous solid dispersions: Experimental and computational study. *Int. J. Pharm.* **2020**, *589*, 119845. [CrossRef]
9. Guedes, F.L.; De Oliveira, B.G.; Hernandes, M.Z.; De Simone, C.A.; Veiga, F.J.B.; De Lima, M.D.C.A.; Pitta, I.R.; Galdino, S.L.; Neto, P.R. Solid dispersions of imidazolidinedione by PEG and PVP polymers with potential antischistosomal activities. *AAPS PharmSciTech* **2011**, *12*, 401–410. [CrossRef]
10. Wilson, V.R.; Lou, X.; Osterling, D.J.; Stolarik, D.F.; Jenkins, G.J.; Nichols, B.L.B.; Dong, Y.; Edgar, K.J.; Zhang, G.G.Z.; Taylor, L.S. Amorphous solid dispersions of enzalutamide and novel polysaccharide derivatives: Investigation of relationships between polymer structure and performance. *Sci. Rep.* **2020**, *10*, 18535. [CrossRef]
11. Barzegar-Jalali, M.; Ghanbarzadeh, S.; Adibkia, K.; Valizadeh, H.; Bibak, S.; Mohammadi, G.; Siahi-Shadbad, M. Development and characterization of solid dispersion of piroxicam for improvement of dissolution rate using hydrophilic carriers. *BioImpacts* **2014**, *4*, 141. [CrossRef]
12. Law, D.; Schmitt, E.A.; Marsh, K.C.; Everitt, E.A.; Wang, W.; Fort, J.J.; Krill, S.L.; Qiu, Y. Ritonavir–PEG 8000 amorphous solid dispersions: In vitro and in vivo evaluations. *J. Pharm. Sci.* **2004**, *93*, 563–570. [CrossRef] [PubMed]
13. Hewlings, S.J.; Kalman, D.S. Curcumin: A review of its effects on human health. *Foods* **2017**, *6*, 92. [CrossRef] [PubMed]
14. Loh, G.O.K.; Tan, Y.T.F.; Peh, K.-K. Enhancement of norfloxacin solubility via inclusion complexation with β-cyclodextrin and its derivative hydroxypropyl-β-cyclodextrin. *Asian J. Pharm. Sci.* **2016**, *11*, 536–546. [CrossRef]
15. Khan, S.; Batchelor, H.; Hanson, P.; Perrie, Y.; Mohammed, A.R. Physicochemical characterisation, drug polymer dissolution and in vitro evaluation of phenacetin and phenylbutazone solid dispersions with polyethylene glycol 8000. *J. Pharm. Sci.* **2011**, *100*, 4281–4294. [CrossRef] [PubMed]
16. Dong, W.; Su, X.; Xu, M.; Hu, M.; Sun, Y.; Zhang, P. Preparation, characterization, and in vitro/vivo evaluation of polymer-assisting formulation of atorvastatin calcium based on solid dispersion technique. *Asian J. Pharm. Sci.* **2018**, *13*, 546–554. [CrossRef]
17. Chaturvedi, K.; Shah, H.S.; Nahar, K.; Dave, R.; Morris, K.R. Contribution of crystal lattice energy on the dissolution behavior of eutectic solid dispersions. *ACS Omega* **2020**, *5*, 9690–9701. [CrossRef]
18. Alonzo, D.E.; Raina, S.; Zhou, D.; Gao, Y.; Zhang, G.G.Z.; Taylor, L.S. Characterizing the impact of hydroxypropylmethyl cellulose on the growth and nucleation kinetics of felodipine from supersaturated solutions. *Cryst. Growth Des.* **2012**, *12*, 1538–1547. [CrossRef]
19. Xie, T.; Taylor, L.S. Dissolution performance of high drug loading celecoxib amorphous solid dispersions formulated with polymer combinations. *Pharm. Res.* **2016**, *33*, 739–750. [CrossRef] [PubMed]
20. Metre, S.; Mukesh, S.; Samal, S.K.; Chand, M.; Sangamwar, A.T. Enhanced biopharmaceutical performance of rivaroxaban through polymeric amorphous solid dispersion. *Mol. Pharm.* **2018**, *15*, 652–668. [CrossRef]

21. Carneiro, S.B.; Costa Duarte, F.Í.; Heimfarth, L.; Siqueira Quintans, J.D.S.; Quintans-Júnior, L.J.; Veiga Júnior, V.F.D.; De Lima, A.N. Cyclodextrin–drug inclusion complexes: In vivo and in vitro approaches. *Int. J. Mol. Sci.* **2019**, *20*, 642. [CrossRef]
22. Konno, H.; Taylor, L.S. Influence of different polymers on the crystallization tendency of molecularly dispersed amorphous felodipine. *J. Pharm. Sci.* **2006**, *95*, 2692–2705. [CrossRef] [PubMed]
23. Konno, H.; Taylor, L.S. The stability, sustained release and cellular antioxidant activity of curcumin nanoliposomes. *Molecules* **2015**, *20*, 14293–14311.
24. Chen, X.; Zou, L.-Q.; Niu, J.; Liu, W.; Peng, S.-F.; Liu, C.-M. Characterization of curcumin/cyclodextrin polymer inclusion complex and investigation on its antioxidant and antiproliferative activities. *Molecules* **2018**, *23*, 1179. [CrossRef] [PubMed]
25. Haroon, K.; Kok, K. Comparative Curcumin Solubility Enhancement Study of ß-Cyclodextrin (ßCD) and its Derivative Hydroxypropyl-ß-Cyclodextrin (HPßCD). *Lat. Am. J. Pharm.* **2013**, *32*, 52–59.
26. Akhlaq, M.; Maryam, F.; Elaissari, A.; Ullah, H.; Adeel, M.; Hussain, A.; Ramzan, M.; Ullah, O.; Danish, M.Z.; Iftikhar, S.; et al. Pharmacokinetic evaluation of quetiapine fumarate controlled release hybrid hydrogel: A healthier treatment of schizophrenia. *Drug Deliv.* **2018**, *25*, 916–927. [CrossRef]
27. Van der Weerd, J.; Kazarian, S.G. Release of poorly soluble drugs from HPMC tablets studied by FTIR imaging and flow-through dissolution tests. *J. Pharm. Sci.* **2005**, *94*, 2096–2109. [CrossRef] [PubMed]
28. El Maghraby, G.M.; Elsergany, R.N. Fast disintegrating tablets of nisoldipine for intra-oral administration. *Pharm. Dev. Technol.* **2014**, *19*, 641–650. [CrossRef] [PubMed]
29. Zhu, W.-F.; Zhu, L.; Li, Z.; Wu, W.-T.; Guan, Y.-M.; Chen, L.-H.; Mao, Z.-X.; Ming, L.-S. The novel use of PVP K30 as templating agent in production of porous lactose. *Pharmaceutics* **2021**, *13*, 814. [CrossRef] [PubMed]
30. Jamadar, S.; Pore, Y.; Sayyad, F. Formation of amorphous telmisartan polymeric microparticles for improvement of physicochemical characteristics. *Part. Sci. Technol.* **2014**, *32*, 512–519. [CrossRef]
31. Rani, N.S.; Sannappa, J.; Demappa, T. Effects of CdCl2 concentration on the structural, thermal and ionic conductivity properties of HPMC polymer electrolyte films. *Ionics* **2015**, *21*, 133–140. [CrossRef]
32. Akhgari, A.; Dezfuli, A.G.; Rezaei, M.; Kiarsi, M.; Abbaspour, M. The design and evaluation of a fast-dissolving drug delivery system for loratadine using the electrospinning method. *Jundishapur J. Nat. Pharm. Prod.* **2016**, *in press*. [CrossRef]
33. Noviza, D.; Halim, A. Preparation and characterization of solid dispersion telmisartan–hydroxypropyl methyl cellulose (HPMC) E5 LV by co-grinding method. *Orient. J. Chem.* **2017**, *33*, 2.
34. Saralkar, P.; Dash, A.K. Alginate nanoparticles containing curcumin and resveratrol: Preparation, characterization, and in vitro evaluation against DU145 prostate cancer cell line. *AAPS PharmSciTech* **2017**, *18*, 2814–2823. [CrossRef] [PubMed]
35. Song, Z.; Yin, J.; Xiao, P.; Chen, J.; Gou, J.; Wang, Y.; Zhang, Y.; Yin, T.; Tang, X.; He, H. Improving breviscapine oral bioavailability by preparing nanosuspensions, liposomes and phospholipid complexes. *Pharmaceutics* **2021**, *13*, 132. [CrossRef] [PubMed]